Supporting Information

Hyper-crosslinked polymeric ionic liquids (HCPILs) based chainmail adsorbents for highly efficient gaseous toluene capture under high humidity

Xiongfei Nie, Lei Zhang, Tao Jiang, Ruina Zhang, Ying Zhou, Quanli Ke, Xiaopo Niu, Zekai Zhang, Huayan Liu, Guokai Cui, and Hanfeng Lu **

Innovation Team of Air Pollution Control, Institute of Catalytic Reaction Engineering, Zhejiang Key Laboratory of Surface and Interface Science and Engineering for Catalysts, State Key Laboratory of Green Chemical Synthesis and Conversion, College of Chemical Engineering, Zhejiang University of Technology, Hangzhou 310014, China.

* Correspondence: chemcgk@163.com (G Cui) luhf@zjut.edu.cn (H Lu).

ORCID: https://orcid.org/0000-0002-7223-2869 (G Cui)

Experimental methods

Materials

Tetraphenylphosphonium bromide ([Ph_4P][Br], 98%, CAS No. 2751-90-8) was obtained from Shanghai Aladdin Biocherrical Technology Co., Ltd. Lithium bis(triluoromethanesultony)imide ($LiTf_2N$, 99.5%, CAS No. 90076-65-6). 1,4-Bis(chloromethyl)benzene (DCX, 98%, CAS No. 623-25-6) and toluene (99.8%, CAS No. 108-88-3) were obtained from Shanghai Macklin Biochemical Co., Ltd. 1,2-bichloroethane（DCE，99%，CAS No. 107-06-2）and ethanol (EtOH, 99.5%, CAS No. 64-17-5) were approached from Shanghai Titan Scientific Co., Ltd. N_2 (99.99%) were supplied from Hangzhou Jingong Gas Co., Ltd.

Synthesis of [Ph_4P][Tf_2N]

[Ph_4P][Br] and $LiTf_2N$ at 1:1 molar ratio were dissolve in water separately and organic phase was immediately obtained after mixing and stirring. DCE was used to dissolve organics. After separating the organic phase using a separatory funnel and washing with deionized water for 3 times to remove LiBr, the crude [Ph_4P][Tf_2N] in DCE was prepared. Then, neat [Ph_4P][Tf_2N] was obtained after removing the DCE and trance of water by rotary evaporation and freeze drying.

Synthesis of Cu-BTC

Cu-BTC was synthesized via a hydrothermal method.[1] Briefly, 2.174 g of $Cu(NO_3)_2 \cdot 3H_2O$ was dissolved in 40 mL deionized water, while 1.05 g of trimesic acid (H_3BTC) was dispersed in 40 mL ethanol. Both solutions were treated by ultrasonication, mixed under stirring, and transferred to a 100 mL Teflon-lined autoclave. The mixture was heated at 393 K for 12 h. The resulting pale blue solid was filtered, washed sequentially with water and ethanol, and vacuum-dried at 423 K overnight to obtain Cu-BTC powder.

Synthesis of Cu-BTC@HCPIL

Three Cu-BTC@HCPILs used in this work were synthesized from IL and Cu-BTC following pre-synthesis methods. Take the synthesis of Cu-BTC@HCPIL-2 as an example. The reactants, Cu-BTC(1 g), [Ph_4P][Tf_2N] (3.0977 g, 5 mmol) and DCX (0.8753 g, 5 mmol), were added in DCE (70

ml) with anhydrous $FeCl_3$ (3.242 g, 20 mmol) as the catalyst. After the reflux reaction at 80 °C under N_2 atmosphere for 24 h, the brown precipitate was collected and washed with ethanol and water until the wash solution is colorless and clear. Cu-BTC@HCPIL was readily obtained after drying the crude product in a vacuum drying oven at 120 ℃ for 24 h, the yield of Cu-BTC@HCPIL-2 was 16.9 %. Other Cu-BTC@HCPIL were obtained using different initial mass ratio (IL: DCX): Cu-BTC) by the same way.

Characterization of Cu-BTC@HCPIL

The N_2 adsorption-desorption isotherms, pore size distributions, and Brunauer-Emmett Teller (BET) surface areas of all Cu-BTC@HCPILs were measured at 77 K on Micromeritics ASAP 2460. The total pore volumes and the micropore volumes were obtained from the N_2 adsorption-desorption isotherms. The average pore sizes and pore size distributions were calculated from the adsorption branches by the non-local density functional theory (NLDFT) method. The surface morphologies and microstructures of Cu-BTC@HCPIL were analyzed by Scanning Electron Microscope (SEM, Gemini 500). Transmission Electron Microscopy (TEM) analysis was performed with a Tecnai G2 F30 S-Twin electron microscope at 300 kV. Fourier transform infrared (FT-IR) spectra of HCPIL@CuBTC were measured on Thermo Scientific Nicolet iS20. The water contact angles were measured using an automatic video contact angle tester (Chengde JY-82C). Prior to conducting measurements, each sample underwent activation at 120 ℃ under reduced pressure for a duration of 3 hours to eliminate any adsorbed water and gases.

Gaseous toluene adsorption

Breakthrough experiments were used to analysis the effect of relative humidity on the adsorption of gaseous toluene on the Cu-BTC@HCPIL. The breakthrough experiment was conducted using a custom-designed gas chromatography (GC, Agilent 8860 GC) workstation for the laboratory. Briefly, the mixture of gaseous toluene and water vapor with carrier gas of air was flowed to the U-tube and the toluene concentration was fixed at about 2000 ppm. The concentration of toluene in the outlet stream was measured and recorded by GC equipped with hydrogen flame ionization detector (FID).

The capacities about equilibrium adsorption (q_e, in mg g^{-1}) were the maximum adsorption capacities when the Cu-BTC@HCPIL stopped adsorption, and q_e could be calculated according to the following equation:[2]

$$q_e = \frac{F \times C_0 \times 10^{-6}}{W}[t_s - \int_0^{t_s} \frac{C_i}{C_0} dt]$$

where F in ml min^{-1} is the total flow rate (F = 30 ml min^{-1}), t in min is adsorption time, t_s in min is the equilibrium time, C_0 in mg m^{-3} is the concentration of toluene in the feed gas stream, C_i in mg m^{-3} is the concentration of toluene in the exit gas stream at t = i, and W in gram is the adsorbent weight.

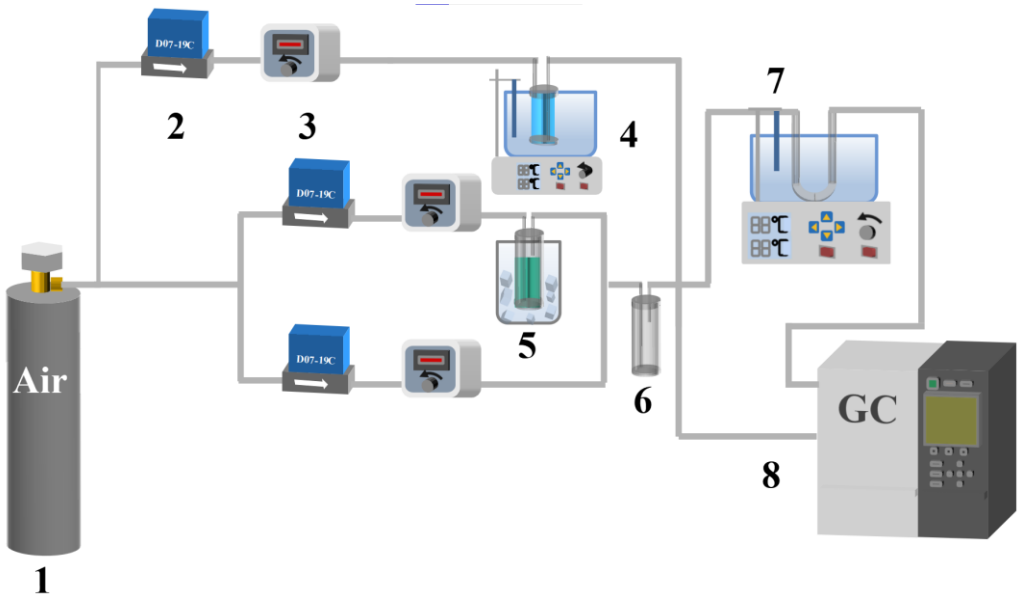

Fig. S1. Schematic diagram of the breakthrough experiments for gaseous toluene adsorption. (1) air cylinder, (2) mass flow meter, (3) flow controller, (4) humidifier, (5) gaseous toluene generator, (6) mixing tank, (7) U-tube, (8) GC with FID.

DFT calculations

DFT calculations were performed with the Gaussian 16, Revision C.01 program package.[3] The geometric optimization of $[Ph_4P]$···Toluene and $[Tf_2N]$···Toluene was carried out by using DFT-D3(BJ)/B3LYP/6–31++G(d, p) methods.[4, 5] The independent gradient model based on Hirshfeld partition (IGMH) analyses was calculated using Multiwfn 3.8 (dev) at DFT-D3(BJ)/B3LYP/6–31++G(d,p) level and drawn with VMD (1.9.4).[6]

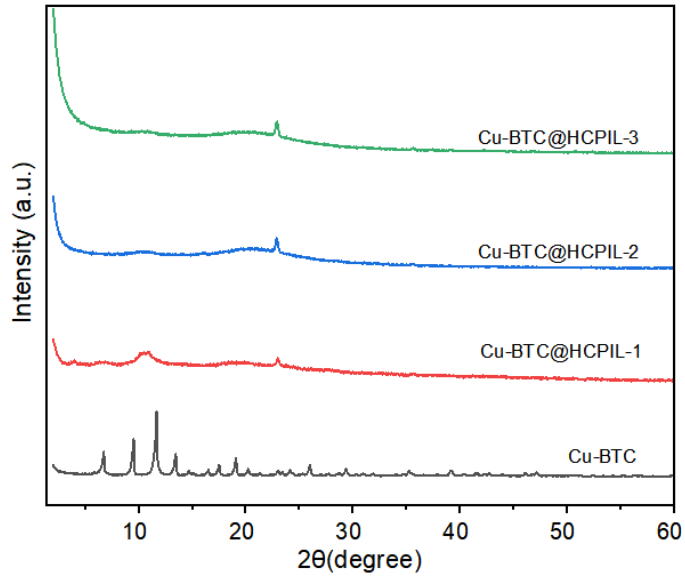

Fig. S2 The XRD patterns (a) of Cu-BTC, Cu-BTC@HCPIL-1, Cu-BTC@HCPIL-2, and Cu-BTC@HCPIL-3;

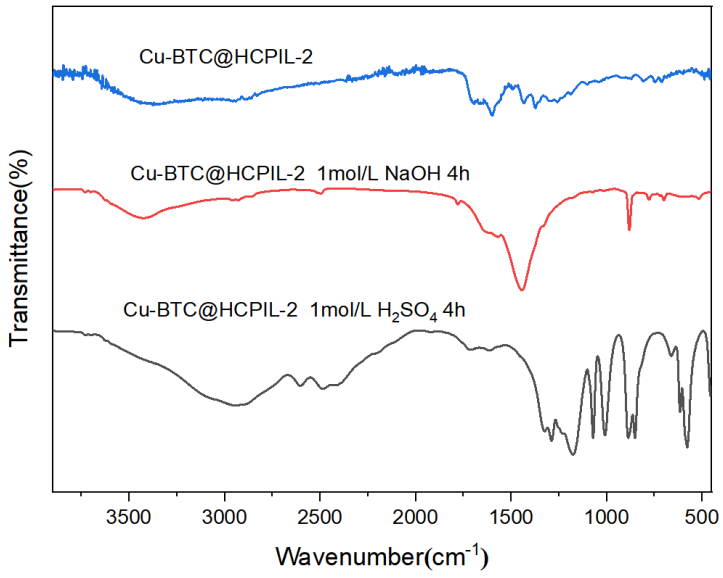

Fig. S3 FT-IR comparison of Cu-BTC@HCPIL-2 and Cu-BTC@HCPIL-2 after 4 hours of treatment with 1 mol/L NaOH and 1 mol/L H_2SO_4 aqueous solutions

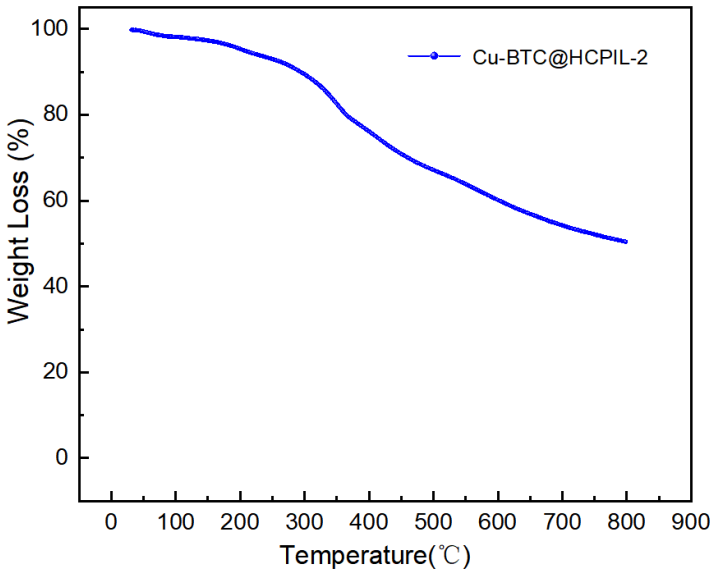

Fig. S4 TGA curve of Cu-BTC@HCPIL-2.

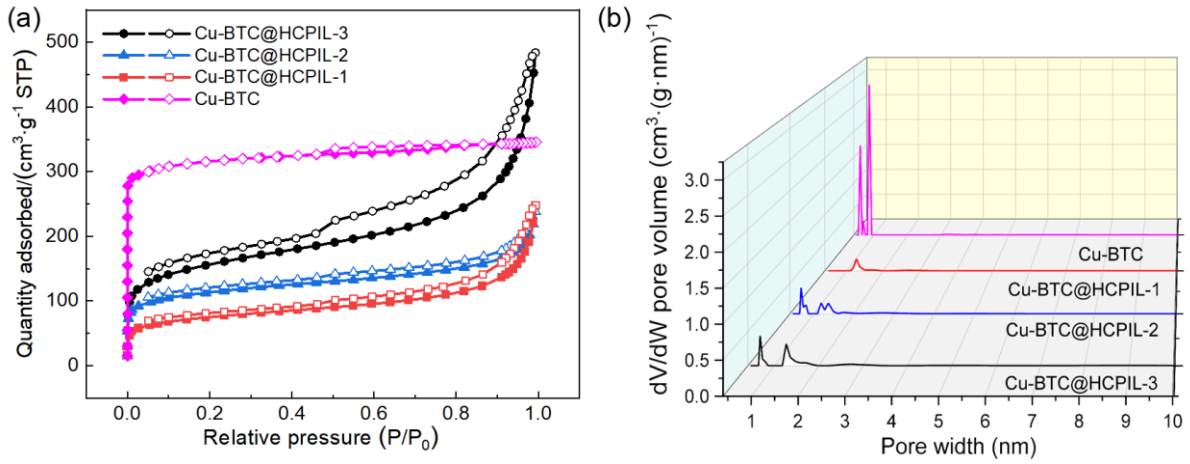

Fig. S5 N_2 adsorption-desorption isotherms at 77 K of (a) and the pore distributions (b) of Cu-BTC, Cu-BTC@HCPIL-1, Cu-BTC@HCPIL-2 and Cu-BTC@HCPIL-3.

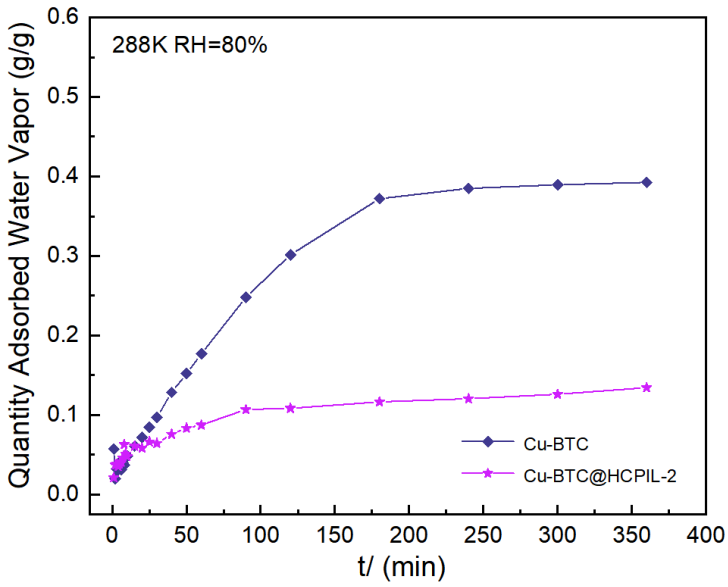

Fig. S6 Time-dependent water vapor adsorption capacity of Cu-BTC and Cu-BTC@HCPIL-2 at 288K, RH= 80 %.

Table S1 Toluene adsorption capacity under different conditions.

Adsorbent	Dry Toluene (mg/g)	Wet Toluene (mg/g)	Condition	Ref.
PSAC-Na-K-N	224	177	313K,80%RH	[7]
PSCC	322	250	298K,80%RH	[8]
PSC-2	365	231	298K,80%RH	[8]
MIL-101	756	189	298K,80%RH	[9]
D-MIL-101-20%	342	289	298K,80%RH	[9]
[Tf_2N]-ILHCP	273	266	298K,80%RH	[10]
Cu-BTC	396	49	298K,80%RH	This work
Cu-BTC@HCPIL-2	339	305	298K,80%RH	This work

References

1. M. Zhang, J. Chen, X. Zhao, X. Mao, C. Li, J. Diwu, G. Wu, Z. Chai and S. Wang, *Angew. Chem., Int. Ed.*, 2024, **63**, e202405213.
2. Q. Ke, Y. Xiong, M. Lu, G. Fang, G. Cui, P. Pan, F. Xiong, T. Wu, K. Huang, J. Min, C. Jin and H. Lu, *Sep. Purif. Technol.*, 2024, **344**, 127268.
3. M. J. Frisch, G. W. Trucks, H. B. Schlegel, G. E. Scuseria, M. A. Robb, J. R. Cheeseman, G. Scalmani, V. Barone, G. A. Petersson, H. Nakatsuji, X. Li, M. Caricato, A. V. Marenich, J. Bloino, B. G. Janesko, R. Gomperts, B. Mennucci, H. P. Hratchian, J. V. Ortiz, A. F. Izmaylov,

J. L. Sonnenberg, Williams, F. Ding, F. Lipparini, F. Egidi, J. Goings, B. Peng, A. Petrone, T. Henderson, D. Ranasinghe, V. G. Zakrzewski, J. Gao, N. Rega, G. Zheng, W. Liang, M. Hada, M. Ehara, K. Toyota, R. Fukuda, J. Hasegawa, M. Ishida, T. Nakajima, Y. Honda, O. Kitao, H. Nakai, T. Vreven, K. Throssell, J. A. Montgomery Jr., J. E. Peralta, F. Ogliaro, M. J. Bearpark, J. J. Heyd, E. N. Brothers, K. N. Kudin, V. N. Staroverov, T. A. Keith, R. Kobayashi, J. Normand, K. Raghavachari, A. P. Rendell, J. C. Burant, S. S. Iyengar, J. Tomasi, M. Cossi, J. M. Millam, M. Klene, C. Adamo, R. Cammi, J. W. Ochterski, R. L. Martin, K. Morokuma, O. Farkas, J. B. Foresman and D. J. Fox, *Journal*, 2016.

4. A. D. Becke, *J. Chem. Phys.*, 1993, **98**, 5648-5652.
5. P. J. Stephens, F. J. Devlin, C. F. Chabalowski and M. J. Frisch, *J. Phys. Chem.*, 1994, **98**, 11623-11627.
6. T. Lu and F. Chen, *J. Comput. Chem.*, 2012, **33**, 580-592.
7. T. Cheng, Y. Bian, J. Li, X. Ma, L. Yang, L. Zhou and H. Wu, *Fuel*, 2023, **334**, 126452.
8. H. Zhang, Z. Yang, E. Cao, Y. Zheng, Q. Ren and Y. Cui, *Chem. Eng. J.*, 2024, **490**, 151817.
9. X. Luan, S. J. Shah, X. Yu, R. Wang, J. Bao, L. Liu, J. Deng, Z. Zhao and Z. Zhao, *Chem. Eng. J.*, 2024, **479**, 147675.
10. X. Nie, X. Qiu, R. Zhang, Q. Ke, H. Liu, X. Zhang, H. Lu, G. Cui and S. Zhang, *Chem. Eng. J.*, 2025, **505**, 159467.